RSC Advances

PAPER

View Article Online
View Journal | View Issue

Cite this: *RSC Adv.*, 2015, **5**, 73926

Structurally simple phenanthroimidazole-based bipolar hosts for high-performance green and red electroluminescent devices†

Kai Wang, Shipan Wang, Jinbei Wei, Yang Miao, Zhenyu Zhang, Zuolun Zhang,* Yu Liu and Yue Wang

Received 23rd July 2015
Accepted 24th August 2015

DOI: 10.1039/c5ra14570h

www.rsc.org/advances

With the aim of developing bipolar host materials, *m*-DPPI with two phenanthroimidazole groups *meta*-linked on a benzene ring and its donor–acceptor-type analogue, *m*-PPPI, with one of the phenanthroimidazole moieties replaced by an electron-withdrawing imidazophenanthroline group have been synthesized. The *meta*-linkage endows these compounds with relatively high triplet energies of *ca.* 2.6 eV for hosting both green and red phosphorescent emitters. The single-carrier devices indicate that both the neat and phosphor-doped films of these compounds have bipolar transporting properties, with relatively higher current densities for the films of *m*-DPPI. Efficient green (maximum efficiencies: 58.5 cd A^{-1}, 67.1 lm W^{-1}, external quantum efficiency (η_{ext}) of 15.5%) and red (maximum efficiencies: 19.7 cd A^{-1}, 26.9 lm W^{-1}, η_{ext} of 11.6%) PhOLEDs have been achieved using *m*-DPPI as the host. The performance of *m*-PPPI-based devices is also high, although a bit lower than that of *m*-DPPI-based devices. Moreover, all the devices exhibit low current-efficiency and η_{ext} roll-off. The simple structures, easy syntheses and high device performance of these compounds are attractive regarding practical applications.

Introduction

Due to the ability of harvesting both electro-generated singlet and triplet excitons to achieve a 100% theoretical internal quantum efficiency, phosphorescent organic light-emitting diodes (PhOLEDs) exhibit great potential in both flat-panel displays and solid-state lighting.[1,2] In PhOLEDs, a doped emitting layer (EML) with a fluorescent host as the matrix for dispersing phosphorescent emitters is usually adopted in order to avoid aggregation-caused luminescence quenching and triplet–triplet annihilation of the phosphors.[3] As a result, the device performance is highly dependent on the properties of host materials. Recently, bipolar transporting hosts able to transport both electrons and holes have drawn considerable attention because they can provide relatively balanced hole and electron fluxes and a large hole–electron recombination zone in EML for improving device performance.[4] One effective strategy for constructing bipolar hosts is incorporating electron-donating and electron-accepting groups into a molecule, as these two components could accept/transport holes and electrons, respectively.[4a,5–8] However, the bipolar host is not limited to the donor–acceptor systems, as a few materials without obvious push–pull structures have also been proved to possess bipolar transporting ability.[4a] Besides the transporting requirements, another generally required character for host materials in PhOLEDs is a relatively large triplet energy for efficient triplet exciton transfer from host to guest and for preventing the reverse transfer.[4a,9,10] In addition, a large triplet energy may make the host suitable for phosphorescent emitters with different emission colours.[11] This is of great importance for full-colour/white OLEDs as it can reduce the varieties of applied materials and thus improve the process stability and reduce the production cost.[11]

Recently, phenanthroimidazole derivatives have attracted increasing attention as blue emitters[12,13] and host materials.[14,15] For this class of hosts, an intriguing feature is that they usually exhibit bipolar transporting character. For example, Yang and coworkers reported a series of phenanthroimidazole/carbazole hybrid bipolar hosts, and the green-emitting devices based on them showed a maximum current efficiency ($\eta_{c,max}$) of 77.6 cd A^{-1}, a maximum power efficiency ($\eta_{p,max}$) of 80.3 lm W^{-1}, and a maximum external quantum efficiency ($\eta_{ext,max}$) of 21%;[14a,b] we also reported a series of bipolar hosts based on metal complexes and organic derivatives of phenanthroimidazole, which can realize high-performance red, green and blue OLEDs.[15] These progresses suggest the great potential of phenanthroimidazole

State Key Laboratory of Supramolecular Structure and Materials, College of Chemistry, Jilin University, Changchun 130012, P. R. China. E-mail: zuolunzhang@jlu.edu.cn

† Electronic supplementary information (ESI) available: TGA and DSC curves and additional photophysical, crystallographic and electroluminescent data. CCDC 1008378. For ESI and crystallographic data in CIF or other electronic format see DOI: 10.1039/c5ra14570h

derivatives as candidates for commercial host materials. However, the research on this class of hosts is still limited. Therefore, the further development is important and attractive.

In this study, we have synthesized two phenanthroimidazole derivatives, *m*-DPPI and *m*-PPPI, with the aim of developing bipolar hosts. *m*-DPPI with two phenanthroimidazole moieties *meta*-linked on a benzene ring has no obvious push–pull character, while by replacing one phenanthroimidazole moiety with more electron-withdrawing imidazophenanthroline,[16] *m*-PPPI possesses a donor–acceptor structure. The *meta*-linkage of two bulky substituents is beneficial to the realization of high triplet energies.[7a,13j,17] The carrier transporting properties and OLED performance of these compounds have been evaluated. In addition, the photophysical, electrochemical and thermal properties of them have also been studied.

Results and discussion

Synthesis and crystal structure

As shown in Scheme 1, both *m*-DPPI and *m*-PPPI were synthesized by one-pot reaction through refluxing the mixture of phenanthrene-9,10-dione/1,10-phenanthroline-5,6-dione, aniline, ammonium acetate and corresponding aromatic aldehyde in acetate acid. The crude products separated by simple workup can be easily purified by vacuum sublimation to afford pure samples suitable for electronic devices. Both compounds were synthesized in good yields (56% for *m*-DPPI and 64% for *m*-PPPI). The simple preparation method is beneficial to the reduction of material cost, which is fairly important for materials' commercial application. The structures of both compounds were fully characterized by NMR spectroscopy, mass spectra and elemental analysis.

To understand the molecular confirmations and reveal the intermolecular packing modes, the growth of single crystals was attempted, and the slab-like crystals of *m*-DPPI has been successfully obtained by slow evaporation of its saturated CH_2Cl_2 solution. The crystal belongs to orthorhombic centrosymmetric space group *Pbcn* with $Z = 4$, and the crystal structure is shown in Fig. 1. In the molecule, the phenanthroimidazole group has a good planarity and shows a dihedral angle of 34.9° with the central benzene ring. Adjacent molecules are stacked *via* two kinds of C–H···π interactions, and there are no C–H···N hydrogen-bonding and π···π interactions in the crystal.

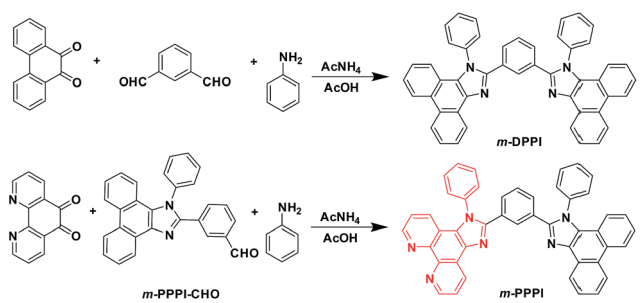

Scheme 1 Synthetic procedure of *m*-DPPI and *m*-PPPI.

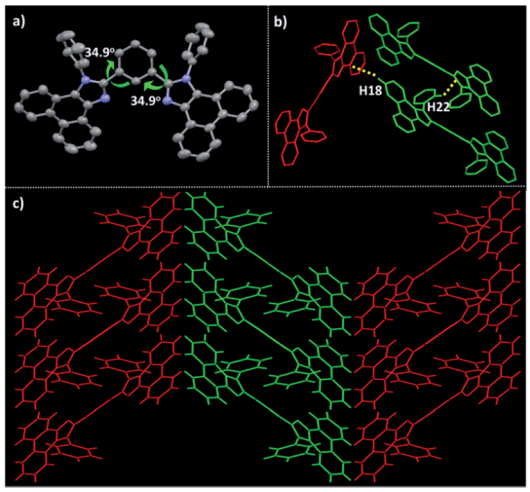

Fig. 1 (a) Molecular structures of *m*-DPPI from single-crystal X-ray diffraction. Element (colour): carbon (gray), nitrogen (blue). Hydrogen atoms are omitted for clarity. Atomic displacement ellipsoids are drawn at 50% probability; (b) intermolecular C–H···π interactions: C–H18···π (H···π-ring centroid = 2.94 Å, H···π-ring plane = 2.81 Å, C···π-ring centroid = 3.77 Å, C–H···π-ring centroid = 149.5°) and C–H22···π (H···π-ring centroid = 2.85 Å, H···π-ring plane = 2.77 Å, C···π-ring centroid = 3.62 Å, C–H···π-ring centroid = 141.0°); (c) molecular packing structure of *m*-DPPI.

Thermal properties

The thermal properties of the compounds were characterized by thermogravimetric analysis (TGA) and differential scanning calorimetry (DSC) under a nitrogen atmosphere at a heating rate of 10 °C min^{-1} (Fig. S1 and S2†). *m*-DPPI and *m*-PPPI exhibit high decomposition temperatures (T_d, corresponding to 5% weight loss) of 477 and 486 °C, respectively, which ensure sufficient stability for vacuum sublimation and device fabrication processes. The melting points (T_m) determined by DSC measurements are 358 °C for *m*-DPPI and 369 °C for *m*-PPPI. Compared with the 1,2-diphenyl-1*H*-phenanthro[9,10-*d*]imidazole (PPI) and its methyl-substituted derivatives, which possess the T_d values of 336–343 °C and T_m values of 194–211 °C,[12a] *m*-DPPI and *m*-PPPI show much higher thermal stability partly due to their significantly increased molecular weight.

Photophysical properties

In CH_2Cl_2 (Fig. 2a), these compounds exhibit similar absorption-spectra profiles and close absorption edges (375 nm for *m*-DPPI and 379 nm for *m*-PPPI). *m*-DPPI displays ultraviolet emission, showing a structured emission spectrum with the maximum (λ_{em}) located at 388 nm. From *m*-DPPI to *m*-PPPI ($\lambda_{em} = 402$ nm), the emission spectrum is slightly red shifted by *ca.* 14 nm and becomes less structured and broader. In the thin-film state (Fig. 2b), the λ_{em} of *m*-DPPI is located at 384 nm, close to that of the CH_2Cl_2 solution. As for *m*-PPPI, the thin-film emission spectrum (λ_{em} = 434 nm) is obviously red-shifted and broader than the solution spectrum, suggesting strong intermolecular interactions in the solid state.[18] The phosphorescence spectra of these compounds measured in 2-MeTHF at

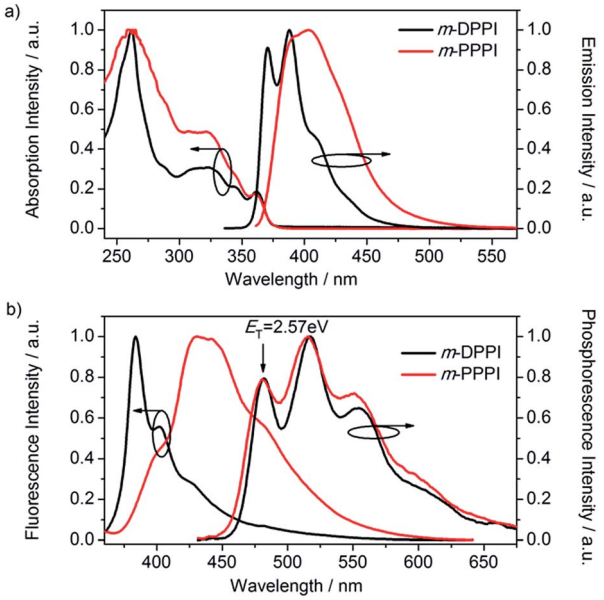

Fig. 2 (a) UV-vis absorption and emission spectra of *m*-DPPI and *m*-PPPI in CH_2Cl_2 (10^{-5} M); (b) emission spectra of *m*-DPPI and *m*-PPPI in thin-film state and their phosphorescence spectra in 2-MeTHF (10^{-5} M) at 77 K.

77 K are very similar (Fig. 2b). The triplet energies (E_T) estimated from the highest-energy vibronic sub-band of the phosphorescence spectra[17,19] are 2.57 eV for both compounds, which is close to the E_T value of classical phosphorescent host CBP (4,4′-bis(*N*-carbazolyl)-1,1′-biphenyl, 2.56 eV)[20] and sufficiently high to host green and red phosphorescent dyes.[4b] We note that the E_T value of these compounds is also quite close to that of PPI ($E_T = 2.61$ eV), indicating that the *meta*-linkage is effective for retaining the triplet energy (Fig. S3†).

Electrochemical properties and theoretical calculations

Cyclic voltammetry (CV) measurements were carried out to estimate the HOMO and LUMO energy levels (Fig. 3). The oxidation onset potentials of *m*-DPPI and *m*-PPPI in CH_2Cl_2 were determined to be 0.80 and 0.82 V (*vs.* ferrocene/ferrocenium), respectively. Correspondingly, the HOMO energy levels were estimated to be −5.90 eV for *m*-DPPI and −5.92 eV for *m*-PPPI by assuming that the HOMO of ferrocene lies 5.1 eV (ref. 21) below vacuum level. Because there is no clear reduction process for these compounds within the electrochemical window of CH_2Cl_2 or even THF and DMF, the LUMO energy levels were deduced from HOMO energies and the optical band gaps determined from the edge of absorption spectra.[12a,g,h,j,14b,15a,22] The deduced LUMO energies are −2.60 and −2.65 eV for *m*-DPPI and *m*-PPPI, respectively.

To gain further insight into the electronic structures of these compounds, density functional theory (DFT) calculations were performed at B3LYP/6-31G(d) level (Fig. 4). The HOMO of *m*-DPPI is distributed on the whole molecule except the N-bonded phenyl groups, while the LUMO is distributed on the C_6H_4 linker and a part of each phenanthroimidazole moiety.

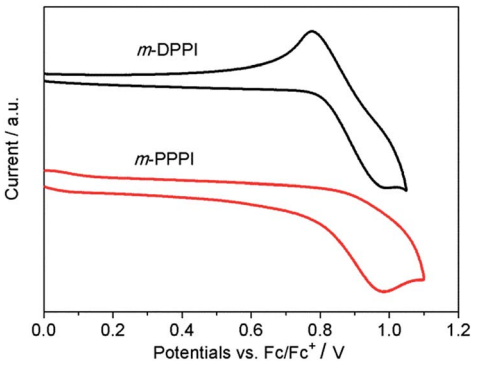

Fig. 3 Cyclic voltammograms of *m*-DPPI and *m*-PPPI in CH_2Cl_2.

For *m*-PPPI, due to the introduction of electron-withdrawing imidazophenanthroline moiety, HOMO and LUMO show clear spatial separation. The HOMO is mainly located on the phenanthroimidazole donor, while the LUMO is mainly dispersed on the imidazophenanthroline acceptor and the C_6H_4 linker. From *m*-DPPI to *m*-PPPI, replacing one phenanthroimidazole group with the imidazophenanthroline group slightly lower the HOMO and LUMO energies (Fig. 4).

Single-carrier devices

To evaluate the carrier injection/transporting properties, we fabricated single-carrier devices with the configurations of [ITO/MoO_3 (10 nm)/*m*-DPPI or *m*-PPPI (60 nm)/MoO_3 (10 nm)/Al (100 nm)] for hole-only devices and [ITO/TPBI (10 nm)/*m*-DPPI or *m*-PPPI (60 nm)/TPBI (10 nm)/LiF (1 nm)/Al (100 nm)] for electron-only devices (Fig. 5). MoO_3 and TPBI (1,3,5-tris(*N*-phenylbenzimidazol-2-yl)benzene) are able to prevent electron injection from the cathode (Al) and hole injection from anode (ITO, indium-tin oxide), respectively, which guarantees the single-carrier injection characteristic of these devices.[23] Since dopant molecules may influence carrier transporting properties, we also fabricated single-carrier devices based on the phosphor-doped films of these compounds (doping 8 wt% of typical green phosphor $Ir(ppy)_3$ or red phosphor $Ir(MDQ)_2(acac)$[24]), with the thickness of each layer unchanged for comparison

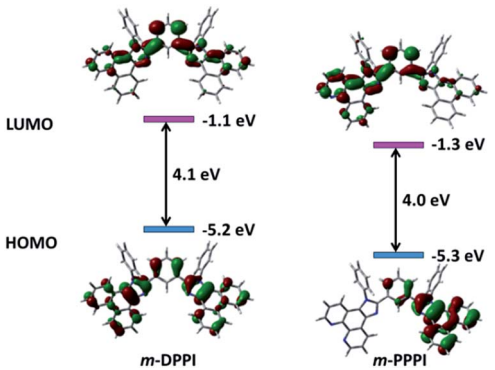

Fig. 4 DFT (B3LYP/6-31G(d)) calculated molecular orbitals and energy levels of *m*-DPPI and *m*-PPPI.

(Fig. 5). The devices of neat *m*-DPPI show good conductivity for holes and electrons as indicated by the availability of large current densities (Fig. 5a and b), suggesting that *m*-DPPI has a bipolar transporting property.[22] Although the single-carrier devices of *m*-PPPI can also conduct holes and electrons, their current densities at the same driving voltage is significantly lower (Fig. 5c and d). Considering the very close HOMO and LUMO energy levels of *m*-DPPI and *m*-PPPI determined by electrochemical data and optical band gaps, the hole injection from MoO_3 and electron injection from TPBI to these compounds should have almost the same energy barrier. Therefore, the much lager current densities of *m*-DPPI-based devices imply a better carrier transporting property of this compound. The relatively poor transporting ability of *m*-PPPI could be related to the specific molecular arrangement in the thin-film state and the more localized HOMO and LUMO distributions (Fig. 4) that may reduce the possibility of intermolecular orbital overlap and therefore lower the charge-transfer integral.[4a,25] Our results further confirm that the non-donor-acceptor systems could also be good bipolar transporting materials. For hole-only devices, the current density at a given driving voltage is decreased when $Ir(ppy)_3$ or $Ir(MDQ)_2(acac)$ is doped into the film of *m*-DPPI or *m*-PPPI. In contrast, the current densities of electron-only devices are increased by doping the Ir-complexes (Fig. 5). Similar influence of phosphor-doping on current densities has been observed before, and the decreased hole current can be explained by the hole-trapping behaviour of the Ir-complexes and the increased electron current should be attributed to additional electron transporting channels formed by the dopants.[26] The devices of doped *m*-DPPI show significantly higher current densities than corresponding devices of doped *m*-PPPI, implying more opportunities for electron–hole recombination in doped *m*-DPPI layer. This feature of doped *m*-DPPI is beneficial to the enhancement of OLED performance when it is used as the emitting layer in electroluminescent (EL) devices.

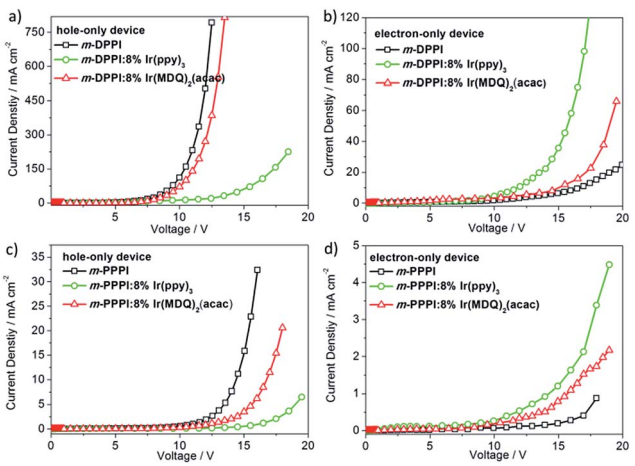

Fig. 5 Current density–voltage characteristics of hole-only and electron-only devices.

Phosphorescent OLEDs

To evaluate the practical utility of *m*-DPPI and *m*-PPPI as host materials, we initially examined the performance of $Ir(ppy)_3$-based green phosphorescent device with the structure of [ITO/MoO_3 (10 nm)/NPB (50 nm)/TCTA (5 nm)/*m*-DPPI (or *m*-PPPI): 8% $Ir(ppy)_3$ (25 nm)/TPBI (30 nm)/LiF (1 nm)/Al (100 nm)] (devices G1 for *m*-DPPI and G2 for *m*-DPPI). NPB (*N*,*N*′-di-(naphthalen-1-yl)-*N*,*N*′-diphenylbenzidine) and TPBI were used as the hole- and electron-transporting layers, respectively; TCTA (4,4′,4″-tri(*N*-carbazolyl)triphenylamine) was used as exciton-blocking layer; MoO_3 and LiF served as hole- and electron-injecting layers, respectively. Fig. 6 depicts the energy level diagram of used materials and molecular structures of the phosphorescent dopants in the devices. The HOMO energies of *m*-DPPI and *m*-PPPI match well with that of TCTA and the LUMO energies match well with that of TPBI, which ensures the efficient carrier injection to the EML. The device performance is summarized in Table 1. The efficiency *versus* current density curves and current density–voltage–luminance (*J*–*V*–*L*) characteristics for the devices are shown in Fig. 7, S4 and S5.† Both devices show a low turn-on voltage of 2.7 V. Device G1 using *m*-DPPI as the host achieves maximum luminance (L_{max}) of 48 016 cd m^{-2}, $\eta_{c,max}$ of 58.5 cd A^{-1}, $\eta_{p,max}$ of 67.1 lm W^{-1} and $\eta_{ext,max}$ of 15.5%. In comparison, device G2 hosted by *m*-PPPI exhibits slightly lower efficiencies with the $\eta_{c,max}$ of 50.7 cd A^{-1}, $\eta_{p,max}$ of 58.9 lm W^{-1} and $\eta_{ext,max}$ of 13.5%. Notably, these devices show low η_c and η_{ext} roll-off. At a brightness of 100 cd m^{-2}, the efficiencies are 57.9 cd A^{-1} and 15.4% for device G1 and 47.5 cd A^{-1} and 12.8% for device G2, without significant decay compared with the maximum values. When the brightness reaches 1000 cd m^{-2}, G1 and G2 still exhibit high η_c values of 54.6 and 43.2 cd A^{-1} and η_{ext} values of 14.6 and 11.5%, respectively. The low efficiency roll-off is of great importance regarding the practical applications in displays and lighting.[3g,5d,27]

Next, the red-emitting OLEDs using 8 wt% $Ir(MDQ)_2(acac)$ as the dopant with the configuration same as that of the green device were fabricated. The turn-on voltages of *m*-DPPI-hosted device, R1, and *m*-PPPI-hosted device, R2, were further reduced to 2.3 V (Table 1). The L_{max} and maximum efficiencies are 42 590 cd m^{-2}, 19.7 cd A^{-1}, 26.9 lm W^{-1} and 11.6% for R1

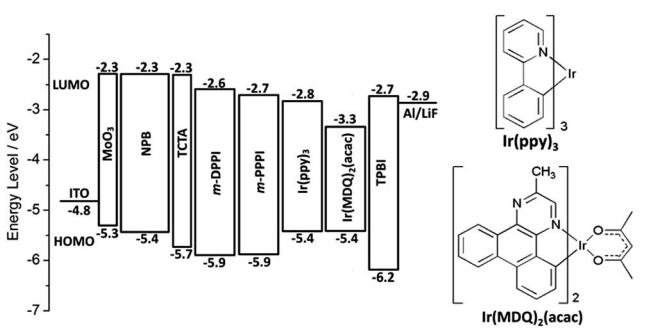

Fig. 6 Energy level diagram of the materials used in EL devices and the chemical structures of the phosphorescent emitters. The HOMO energy levels of *m*-DPPI and *m*-PPPI are calculated from the electrochemical data and the LUMO levels of both compounds are deduced from the HOMO levels and the optical band gaps.

Table 1 Electroluminescent properties of the devices[a]

	Dopant	V_{on}/V	L_{max}/cd m^{-2}	η_c[b]/cd A^{-1}	η_p[b]/lm W^{-1}	η_{ext}[b]/%	CIE (x, y)[c]
G1	Ir(ppy)$_3$	2.7	48 016	58.5, 57.9, 54.6	67.1, 60.4, 41.5	15.5, 15.4, 14.6	0.32, 0.61
G2	Ir(ppy)$_3$	2.7	48 467	50.7, 47.5, 43.2	58.9, 44.0, 29.4	13.5, 12.8, 11.5	0.30, 0.63
R1	Ir(MDQ)$_2$(acac)	2.3	42 590	19.7, 17.1, 16.6	26.9, 17.8, 12.0	11.6, 11.2, 10.5	0.64, 0.36
R2	Ir(MDQ)$_2$(acac)	2.3	37 683	14.6, 14.3, 13.2	16.8, 11.4, 7.02	12.8, 12.6, 10.8	0.64, 0.36

[a] Abbreviation: V_{on}: turn-on voltage; L_{max}: maximum luminance; η_c: current efficiency; η_p: power efficiency; η_{ext}: external quantum efficiency. [b] Values given in the order of maximum, value at 100 cd m^{-2} and value at 1000 cd m^{-2}. [c] Measured at 100 cd m^{-2}.

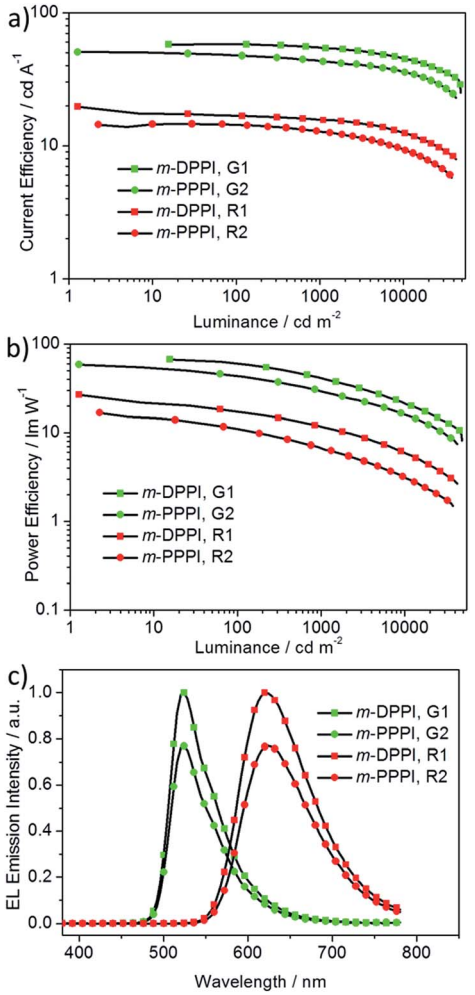

Fig. 7 Current efficiency (a) and power efficiency (b) *versus* luminance curves, and EL spectra (c) of the devices.

(Fig. 7, S4 and S5†). From R1 to R2, the $\eta_{c,max}$ and $\eta_{p,max}$ are decreased to 14.6 cd A^{-1} and 16.8 lm W^{-1}, and the $\eta_{ext,max}$ is only slightly influenced. It is worth noting that the power efficiency of device R1 is comparable with the best values reported for red-emitting PhOLEDs.[3f,28] R1 and R2 also exhibit low η_c and η_{ext} roll-off (Table 1). For example, R1 has the η_c values of 17.1 and 16.6 cd A^{-1} and η_{ext} values of 11.2 and 10.5% at 100 and 1000 cd m^{-2}, respectively.

All the devices display pure green or red emission from the dopant and there isn't residual emission from the host, indicating the complete energy transfer from host to dopant (Fig. 7c). Given the same triplet energy and close HOMO and LUMO energies of *m*-DPPI and *m*-PPPI, the relatively higher performance of *m*-DPPI-based devices should be partly ascribed to a better carrier transporting ability of the doped *m*-DPPI film as suggested by the single-carrier devices. The bipolar transporting property of the doped emitting layer results in a large recombination zone for electrons and holes. This can reduce the triplet–triplet annihilation and triplet-polaron quenching and thus reduce the efficiency roll-off at high luminance.[26,29]

Conclusion

In summary, two phenanthroimidazole-based host materials, *m*-DPPI and *m*-PPPI, have been designed and synthesized. These compounds exhibit bipolar transporting ability, regardless of whether they have donor–acceptor structures. Moreover, they possess high triplet energies of *ca.* 2.6 eV, which enable them to act as hosts for both the green and red phosphors. By using them as host materials, efficient green and red PhOLEDs have been achieved. The performance of *m*-DPPI-based devices is higher, partly due to the better transporting ability of doped *m*-DPPI layer. In addition, all the devices show low efficiency roll-off with slightly changed η_c and η_{ext} values within the brightness range of 100–1000 cd m^{-2}. The facile syntheses, the ability to host multicolour dopants and the good device performance of these compounds are all valuable merits with respect to commercial applications. Our studies further confirm that phenanthroimidazole is an excellent building block for bipolar hosts and both the donor–acceptor and non-donor–acceptor systems based on it could be good bipolar transporting materials.

Experimental

General information

MoO_3, NPB, TCTA, TPBI, LiF, *n*-Bu_4NPF_6 and the starting materials for organic syntheses were obtained from commercial sources. All of the organic materials used for device fabrication were purified by vacuum sublimation prior to use. The starting materials for syntheses were used as received. All synthetic reactions were carried out under a nitrogen atmosphere by using Schlenk techniques. ^{1}H NMR spectra were measured on Bruker Avance 500 MHz spectrometer with tetramethylsilane (TMS) as the internal standard. Mass spectra were recorded on a Shimadzu AXIMA-CFR MALDI-TOF mass spectrometer.

Elemental analyses were performed on a flash EA 1112 analyser. UV-vis absorption spectra were recorded by a Shimadzu UV-2550 spectrophotometer. The emission spectra were recorded by a Shimadzu RF-5301 PC spectrometer. DSC measurements were performed on a NETZSCH DSC204 instrument at a heating rate of 10 °C min^{-1} under a nitrogen atmosphere. TGA measurements were performed on a TA Q500 thermogravimeter by measuring their weight loss while heating at a rate of 10 °C min^{-1} under nitrogen. Electrochemical measurements were performed with a BAS 100W Bioanalytical electrochemical work station with a scan rate of 100 mV s^{-1}. A three-electrode cell configuration was employed for the measurement: a platinum disk as the working electrode, a platinum wire as the counter electrode, and an Ag/Ag^+ electrode as the reference electrode. The oxidation potentials were measured in dichloromethane solution containing 0.1 M of n-Bu_4NPF_6 as the supporting electrolyte at a scan rate of 100 mV s^{-1}.

Single-crystal structure

Diffraction data were collected on a Rigaku RAXIS-PRID diffractometer using the ω-scan mode with graphite-monochromator Mo Kα radiation. The structure was solved with direct methods using the SHELXTL programs and refined with full-matrix least-squares on F^2.[30] Non-hydrogen atoms were refined anisotropically. The positions of hydrogen atoms were calculated and refined isotropically. ESI.†

Theoretical calculations

The ground state geometries were optimized by the density functional theory (DFT)[31] method with the Becke three-parameter hybrid exchange and the Lee–Yang–Parr correlation functional[32] (B3LYP) and 6-31G(d) basis set using the Gaussian 03 software package.[33] The molecular structure of *m*-DPPI as determined by X-ray crystallography was used as the input for optimizing ground-state geometries; by changing two carbon atoms with nitrogen atoms, the geometry of *m*-PPPI was optimized.

Fabrication and characterization of OLEDs and single-carrier devices

Before device fabrication, the ITO-coated glass substrates were pre-cleaned by sonication successively in a detergent solution, acetone, methanol, and deionized water and then treated with plasma for 2 min. The devices were prepared in vacuum at a pressure of 5×10^{-6} Torr. Organic layers, MoO_3 and LiF were deposited onto the substrate at a rate of 0.3–0.5 Å s^{-1}. The Al electrode was deposited at a rate of 10 Å s^{-1}. Thicknesses of the material layer were controlled using a quartz crystal thickness monitor. The electrical characteristics of the OLEDs and single-carrier devices were measured with a Keithley 2400 source meter. The EL spectra and luminance of the OLEDs were obtained using a PR650 spectrometer. All measurements were carried out on the devices without encapsulations in ambient atmosphere under dark.

Synthesis

1,3-Bis(1-phenyl-1*H*-phenanthro[9,10-*d*]imidazol-2-yl)benzene (*m*-DPPI). A mixture of phenanthrene-9,10-dione (2.0 g, 9.6 mmol), isophthalaldehyde (0.64 g, 4.8 mmol), aniline (4.46 g, 48.0 mmol), ammonium acetate (2.96 g, 38.4 mmol) and glacial acetic acid (40 mL) was heated at 123 °C for 3 h. After cooled to room temperature, the reaction mixture was poured into distilled water under stirring. The resulting precipitate was filtered out and washed with water to give the crude product, which was further purified by vacuum sublimation to produce pure *m*-DPPI (1.78 g, 56%). ^{1}H NMR (500 MHz, DMSO-d_6): δ 8.95 (d, J = 8.0 Hz, 2H), 8.90 (d, J = 8.0 Hz, 2H), 8.72 (d, J = 8.0 Hz, 2H), 8.10 (s, 1H), 7.83 (t, J = 7.0 Hz, 2H), 7.75–7.69 (m, 12H),7.58 (t, J = 7.0 Hz, 2H), 7.46 (d, J = 7.5 Hz, 2H), 7.36 (t, J = 7.5 Hz, 2H), 7.28 (t, J = 8.0 Hz, 1H), 7.09 (d, J = 8.0 Hz, 2H). MS m/z: 662.1 $[M]^+$ (calcd: 662.3). Anal. calcd (%) for $C_{48}H_{30}N_4$: C, 86.98; H, 4.56; N, 8.45. Found: C, 86.76; H, 4.47; N, 8.53.

3-(1-Phenyl-1*H*-phenanthro[9,10-*d*]imidazol-2-yl)benzaldehyde (*m*-PPI-CHO). A mixture of phenanthrene-9,10-dione (0.50 g, 2.4 mmol), isophthalaldehyde (0.96 g, 7.2 mmol), aniline (2.23 g, 24 mmol), ammonium acetate (1.48 g, 19.2 mmol) and glacial acetic acid (30 mL) was heated at 123 °C for 3 h. After cooled to room temperature, the reaction mixture was poured into distilled water under stirring. The resulting precipitate was filtered out and washed with water to give the crude product, which was further purified by vacuum sublimation to produce *m*-PPI-CHO (726 mg, 76%). ^{1}H NMR (500 MHz, DMSO-d_6): δ 9.99 (s, 1H), 8.95 (d, J = 8.5 Hz, 1H), 8.90 (d, J = 8.5 Hz, 1H), 8.72 (d, J = 8.0 Hz, 1H), 8.16 (s, 1H), 7.93 (d, J = 8.0 Hz, 1H), 7.84–7.70 (m, 8H),7.56 (t, J = 7.5 Hz, 2H), 7.36 (t, J = 7.5 Hz, 1H), 7.13 (d, J = 8.0 Hz, 1H). MS m/z: 398.0 $[M]^+$ (calcd: 398.1). Anal. calcd (%) for $C_{28}H_{18}N_2O$: C, 84.40; H, 4.55; N,7.03. Found: C, 84.66; H, 4.47; N, 7.23.

1-Phenyl-2-(3-(1-phenyl-1*H*-phenanthro[9,10-*d*]imidazol-2-yl)-phenyl)-1*H*-imidazo[4,5-*f*][1,10]phenanthroline (*m*-PPPI). The procedure is similar to that for synthesizing *m*-DPPI except that *m*-PPI-CHO and 1,10-phenanthroline-5,6-dione were used as the reactants instead of isophthalaldehyde and phenanthrene-9,10-dione, respectively. *m*-PPPI was obtained in a yield of 64%. ^{1}H NMR (500 MHz, DMSO-d_6): δ 9.28 (d, J = 4.5 Hz, 1H), 9.06 (d, J = 8.0 Hz, 1H), 8.98 (d, J = 4.5 Hz, 1H), 8.95 (d, J = 8.0 Hz,1H), 8.90 (d, J = 8.0 Hz, 1H), 8.71 (d, J = 8.0 Hz, 1H), 8.15 (s, 1H), 7.93 (dd, J = 8.5, 4.5 Hz, 1H), 7.84–7.69 (m, 12H), 7.58 (t, J = 8 Hz, 1H), 7.53–7.46 (m, 3H), 7.39–7.34 (m, 2H), 7.30 (t, J = 8 Hz, 1H), 7.09 (d, J = 7.5 Hz, 1H). MS m/z: 664.3 $[M]^+$ (calcd: 664.2). Anal. calcd (%) for $C_{46}H_{28}N_6$: C, 83.11; H, 4.25; N, 12.64. Found: C, 83.36; H, 4.47; N, 12.43.

Acknowledgements

This work was supported by the National Basic Research Program of China (2015CB655000), the National Natural Science Foundation of China (91333201 and 21221063) and Program for Chang Jiang Scholars and Innovative Research Team in University (No. IRT101713018).

Notes and references

1 (*a*) M. A. Baldo, D. F. O'Brien, Y. You, A. Shoustikov, S. Sibley, M. E. Thompson and S. R. Forrest, *Nature*, 1998, **395**, 151; (*b*) M. A. Baldo, S. Lamansky, P. E. Burrows, M. E. Thompson and S. Forrest, *Appl. Phys. Lett.*, 1999, **75**, 4; (*c*) C. Adachi, M. A. Baldo, D. Brien, M. E. Thompson and S. R. Forrest, *J. Appl. Phys.*, 2001, **90**, 5048; (*d*) Y. Sun, N. C. Giebink, H. Kanno, B. Ma, M. E. Thompson and S. R. Forrest, *Nature*, 2006, **440**, 908; (*e*) B. W. D'Andrade and S. R. Forrest, *Adv. Mater.*, 2004, **16**, 1585; (*f*) S. Reineke, F. Lindner, G. Schwartz, N. Seidler, K. Walzer, B. Lussem and K. Leo, *Nature*, 2009, **459**, 234; (*g*) K. Walzer, B. Maenning, M. Pfeiffer and K. Leo, *Chem. Rev.*, 2007, **107**, 1233.

2 (*a*) K. T. Kamtekar, A. P. Monkman and M. R. Bryce, *Adv. Mater.*, 2010, **22**, 572; (*b*) Y. Zheng, A. S. Batsanov, M. A. Fox, H. A. Al-Attar, K. Abdullah, V. Jankus, M. R. Bryce and A. P. Monkman, *Angew. Chem., Int. Ed.*, 2014, **53**, 11616; (*c*) G. Li, D. Zhu, T. Peng, Y. Liu, Y. Wang and M. R. Bryce, *Adv. Funct. Mater.*, 2014, **24**, 7420; (*d*) G. M. Farinola and R. Ragni, *Chem. Soc. Rev.*, 2011, **40**, 3467; (*e*) M. C. Gather, A. Köhnen and K. Meerholz, *Adv. Mater.*, 2011, **23**, 233; (*f*) G. Zhou, C.-L. Ho, W.-Y. Wong, Q. Wang, D. Ma, L. Wang, Z. Lin, T. B. Marder and A. Beeby, *Adv. Funct. Mater.*, 2008, **18**, 499; (*g*) T. Peng, H. Bi, Y. Liu, Y. Fan, H. Gao, Y. Wang and Z. Hou, *J. Mater. Chem.*, 2009, **19**, 8072; (*h*) T. Peng, G. Li, K. Ye, C. Wang, S. Zhao, Y. Liu, Z. Hou and Y. Wang, *J. Mater. Chem. C*, 2013, **1**, 2920; (*i*) T. Peng, Y. Yang, H. Bi, Y. Liu, Z. Hou and Y. Wang, *J. Mater. Chem.*, 2011, **21**, 3551; (*j*) X. Wang, S. L. Gong, D. Song, Z. H. Lu and S. Wang, *Adv. Funct. Mater.*, 2014, **24**, 7257; (*k*) X. Wang, Y.-L. Chang, J. S. Lu, T. Zhang, Z. H. Lu and S. Wang, *Adv. Funct. Mater.*, 2014, **24**, 1911; (*l*) C. Jiang, W. Yang, J. Peng, S. Xiao and Y. Cao, *Adv. Mater.*, 2004, **16**, 537; (*m*) T. Yu, Y. Cao, W. Su, C. Zhang, Y. Zhao, D. Fan, M. Huang, K. Yue and S. Z. D. Cheng, *RSC Adv.*, 2014, **4**, 554.

3 (*a*) S.-J. Su, H. Sasabe, T. I. Takeda and J. Kido, *Chem. Mater.*, 2008, **20**, 1691; (*b*) M. A. Baldo, C. Adachi and S. R. Forrest, *Phys. Rev. B: Condens. Matter Mater. Phys.*, 2000, **62**, 10967; (*c*) D. H. Kim, N. S. Cho, H.-Y. Oh, J. H. Yang, W. S. Jeon, J. S. Park, M. C. Suh and J. H. Kwon, *Adv. Mater.*, 2011, **23**, 2721; (*d*) H. Fukagawa, T. Shimizu, H. Hanashima, Y. Osada, M. Suzuki and H. Fujikake, *Adv. Mater.*, 2012, **24**, 5099; (*e*) J. Kwak, Y.-Y. Lyu, H. Lee, B. Choi, K. Char and C. Lee, *J. Mater. Chem.*, 2012, **22**, 6351; (*f*) C.-H. Fan, P. Sun, T.-H. Su and C.-H. Cheng, *Adv. Mater.*, 2011, **23**, 2981; (*g*) Y.-C. Zhu, L. Zhou, H.-Y. Li, Q.-L. Xu, M.-Y. Teng, Y.-X. Zheng, J.-L. Zuo, H.-J. Zhang and X.-Z. You, *Adv. Mater.*, 2011, **23**, 4041.

4 (*a*) L. Duan, J. Qiao, Y. Sun and Y. Qiu, *Adv. Funct. Mater.*, 2011, **23**, 1137; (*b*) Y. Tao, C. Yang and J. Qin, *Chem. Soc. Rev.*, 2011, **40**, 2943.

5 (*a*) S. O. Jeon, K. S. Yook, C. W. Joo and J. Y. Lee, *Adv. Funct. Mater.*, 2009, **19**, 3644; (*b*) M. Guan, Z. Chen, Z. Bian, Z. Liu, Z. Gong, W. Baik, H. Lee and C. Huang, *Org. Electron.*, 2006, **7**, 330; (*c*) L. Zeng, T. Y.-H. Lee, P. B. Merkel and S. H. Chen, *J. Mater. Chem.*, 2009, **19**, 8772; (*d*) C.-H. Chang, M.-C. Kuo, W.-C. Lin, Y.-T. Chen, K.-T. Wong, S.-H. Chou, E. Mondal, R. C. Kwong, S. Xia, T. Nakagawa and C. Adachi, *J. Mater. Chem.*, 2012, **22**, 3832; (*e*) D. Wagner, S. T. Hoffmann, U. Heinemeyer, I. Münster, A. Köhler and P. Strohriegl, *Chem. Mater.*, 2013, **25**, 3758; (*f*) H.-G. Jang, W. Song, J. Y. Lee and S.-H. Hwang, *RSC Adv.*, 2015, **5**, 17030; (*g*) Y. Zhang, W. Haske, D. Cai, S. Barlow, B. Kippelen and S. R. Marder, *RSC Adv.*, 2013, **3**, 23514.

6 (*a*) Y. Tao, Q. Wang, L. Ao, C. Zhong, C. Yang, J. Qin and D. Ma, *J. Phys. Chem. C*, 2010, **114**, 601; (*b*) D. Yu, F. Zhao, C. Han, H. Xu, J. Li, Z. Zhang, Z. Deng, D. Ma and P. Yan, *Adv. Mater.*, 2012, **24**, 509; (*c*) C. Fan, F. Zhao, P. Gan, S. Yang, T. Liu, C. Zhong, D. Ma, J. Qin and C. Yang, *Chem.–Eur. J.*, 2012, **18**, 5510.

7 (*a*) Z. Ge, T. Hayakawa, S. Ando, M. Ueda, T. Akiike, H. Miyamoto, T. Kajita and M. Kakimoto, *Org. Lett.*, 2008, **10**, 421; (*b*) Z. Gao, M. Luo, X. Sun, H. Tam, M. Wong, B. Mi, P. Xia, K. Cheah and C. Chen, *Adv. Mater.*, 2009, **21**, 688.

8 (*a*) M. Rothmann, S. Haneder, E. Como, C. Lennartz, C. Schildknecht and P. Strohriegl, *Chem. Mater.*, 2010, **22**, 2403; (*b*) A. Padmaperuma, L. Sapochak and P. Burrows, *Chem. Mater.*, 2006, **18**, 2389; (*c*) S. Jeon, K. Yook, C. Joo and J. Lee, *Adv. Mater.*, 2010, **22**, 1872; (*d*) C. Han, Z. Zhang, H. Xu, J. Li, G. Xie, R. Chen, Y. Zhao and W. Huang, *Angew. Chem., Int. Ed.*, 2012, **51**, 10104; (*e*) A. Wada, T. Yasuda, Q. Zhang, Y. Yang, I. Takasu, S. Enomoto and C. Adachi, *J. Mater. Chem. C*, 2013, **1**, 2404.

9 A. Chaskar, H.-F. Chen and K.-T. Wong, *Adv. Mater.*, 2011, **23**, 3876.

10 (*a*) J. Ding, B. Zhang, J. Lü, Z. Xie, L. Wang, X. Jing and F. Wang, *Adv. Mater.*, 2009, **21**, 4983; (*b*) J. Ding, Q. Wang, L. Zhao, D. Ma, L. Wang, X. Jing and F. Wang, *J. Mater. Chem.*, 2010, **20**, 8126; (*c*) X. Wang, S. Wang, Z. Ma, J. Ding, L. Wang, X. Jing and F. Wang, *Adv. Funct. Mater.*, 2014, **24**, 3413; (*d*) S. Shao, J. Ding, T. Ye, Z. Xie, L. Wang, X. Jing and F. Wang, *Adv. Mater.*, 2011, **23**, 3570.

11 (*a*) K. Wang, S. Wang, J. Wei, S. Chen, D. Liu and Y. Liu, *J. Mater. Chem. C*, 2014, **2**, 6817; (*b*) S. Gong, Y. Chen, J. Luo, C. Yang, C. Zhong, J. Qin and D. Ma, *Adv. Funct. Mater.*, 2011, **21**, 1168; (*c*) Q. Wang, J. Ding, D. Ma, Y. Cheng, L. Wang, X. Jing and F. Wang, *Adv. Funct. Mater.*, 2009, **19**, 84; (*d*) H.-H. Chou and C.-H. Cheng, *Adv. Mater.*, 2010, **22**, 2468; (*e*) Y.-L. Chang, S. Yin, Z. Wang, M. G. Helander, J. Qiu, L. Chai, Z. Liu, G. D. Scholes and Z. Lu, *Adv. Funct. Mater.*, 2013, **23**, 705; (*f*) Y. Qian, Y. Ni, S. Yue, W. Li, S. Chen, Z. Zhang, L. Xie, M. Sun, Y. Zhao and W. Huang, *RSC Adv.*, 2015, **5**, 29828.

12 (*a*) Y. Yuan, D. Li, X. Zhang, X. Zhao, Y. Liu, J. Zhang and Y. Wang, *New J. Chem.*, 2011, **35**, 1534; (*b*) Y. Zhang, S.-L. Lai, Q.-X. Tong, M.-Y. Chan, T.-W. Ng, Z.-C. Wen, G.-Q. Zhang, S.-T. Lee, H.-L. Kwonge and C.-S. Lee, *J. Mater. Chem.*, 2011, **21**, 8206; (*c*) Y. Zhang, S.-L. Lai, Q.-X. Tong, M.-F. Lo, T.-W. Ng, M.-Y. Chan, Z.-C. Wen,

J. He, K.-S. Jeff, X.-L. Tang, W.-M. Liu, C.-C. Ko, P.-F. Wang and C.-S. Lee, *Chem. Mater.*, 2012, **24**, 61; (*d*) Y. Yuan, J.-X. Chen, F. Lu, Q.-X. Tong, Q.-D. Yang, H.-W. Mo, T.-W. Ng, F.-L. Wong, Z.-Q. Guo, J. Ye, Z. Chen, X.-H. Zhang and C.-S. Lee, *Chem. Mater.*, 2013, **25**, 4957; (*e*) C.-J. Kuo, T.-Y. Li, C.-C. Lien, C.-H. Liu, F.-I. Wu and M.-J. Huang, *J. Mater. Chem.*, 2009, **19**, 1865; (*f*) Y.-N. Yan, W.-L. Pan and H.-C. Song, *Dyes Pigm.*, 2010, **86**, 249; (*g*) S. Zhuang, R. Shangguan, H. Huang, G. Tu, L. Wang and X. Zhu, *Dyes Pigm.*, 2014, **101**, 93; (*h*) S. Zhuang, R. Shangguan, J. Jin, G. Tu, L. Wang, J. Chen, D. Ma and X. Zhu, *Org. Electron.*, 2012, **13**, 3050; (*i*) D. Kumar, K. R. Thomas, C. C. Lin and J. H. Jou, *Chem.–Asian J.*, 2013, **8**, 2111; (*j*) B. Wang, G. Mu, J. Tan, Z. Lei, J. Jin and L. Wang, *J. Mater. Chem. C*, 2015, **3**, 7709.

13 (*a*) Z. Wang, P. Lu, S. Chen, Z. Gao, F. Shen, W. Zhang, Y. Xu, H. S. Kwokb and Y. Ma, *J. Mater. Chem.*, 2011, **21**, 5451; (*b*) W. Li, D. Liu, F. Shen, D. Ma, Z. Wang, T. Feng, Y. Xu, B. Yang and Y. Ma, *Adv. Funct. Mater.*, 2012, **22**, 2797; (*c*) Z. Wang, P. Lu, S. Chen, Z. Gao, F. Shen, W. Zhang, Y. Xu, H. S. Kwok and Y. Ma, *J. Mater. Chem.*, 2011, **21**, 5451; (*d*) Z. Wang, Z. Gao, S. Xue, Y. Liu, W. Zhang, C. Gu, F. Shen, P. Lu and Y. Ma, *Polym. Bull.*, 2012, **69**, 273; (*e*) Z. M. Wang, X. H. Song, Z. Gao, D. W. Yu, X. J. Zhang, P. Lu, F. Z. Shen and Y. G. Ma, *RSC Adv.*, 2012, **2**, 9635; (*f*) Z. Wang, Y. Feng, H. Li, Z. Gao, X. Zhang, P. Lu, P. Chen, Y. Ma and S. Liu, *Phys. Chem. Chem. Phys.*, 2014, **16**, 10837; (*g*) Z. Gao, G. Cheng, F. Shen, S. Zhang, Y. Zhang, P. Lu and Y. Ma, *Laser Photonics Rev.*, 2014, **8**, L6; (*h*) Z. Gao, Y. Liu, Z. Wang, F. Shen, H. Liu, G. Sun, L. Yao, Y. Lv, P. Lu and Y. Ma, *Chem.–Eur. J.*, 2013, **19**, 2602; (*i*) Z. Wang, Y. Feng, S. Zhang, Y. Gao, Z. Gao, Y. Chen, X. Zhang, P. Lu, B. Yang, P. Chen, Y. Ma and S. Liu, *Phys. Chem. Chem. Phys.*, 2014, **16**, 20772; (*j*) H. Liu, Q. Bai, L. Yao, H. Zhang, H. Xu, S. Zhang, W. Li, Y. Gao, J. Li, P. Lu, H. Wang, B. Yang and Y. Ma, *Chem. Sci.*, 2015, **6**, 3797.

14 (*a*) H. Huang, Y. Wang, S. Zhuang, X. Yang, L. Wang and C. Yang, *J. Phys. Chem. C*, 2012, **116**, 19458; (*b*) H. Huang, Y. Wang, B. Wang, S. Zhuang, B. Pan, X. Yang, L. Wang and C. Yang, *J. Mater. Chem. C*, 2013, **1**, 5899; (*c*) X. Zhang, J. Lin, X. Ouyanga, Y. Liu, X. Liu and Z. Ge, *J. Photochem. Photobiol., A*, 2013, **268**, 37.

15 (*a*) K. Wang, F. Zhao, C. Wang, S. Chen, D. Chen, H. Zhang, Y. Liu, D. Ma and Y. Wang, *Adv. Funct. Mater.*, 2013, **23**, 2672; (*b*) K. Wang, S. Wang, J. Wei, Y. Miao, Y. Liu and Y. Wang, *Org. Electron.*, 2014, **15**, 3211; (*c*) C. Li, S. Wang, W. Chen, J. Wei, G. Yang, K. Ye, Y. Liu and Y. Wang, *Chem. Commun.*, 2015, **51**, 10632; (*d*) D. Liu, M. Du, D. Chen, K. Ye, Z. Zhang, Y. Liu and Y. Wang, *J. Mater. Chem. C*, 2015, **3**, 4394; (*e*) K. Wang, S. Wang, J. Wei, S. Chen, D. Liu, Y. Liu and Y. Wang, *J. Mater. Chem. C*, 2014, **2**, 6817.

16 R. M. F. Batista, S. P. G. Costa, M. Belsley, C. Lodeiro and M. M. M. Raposo, *Tetrahedron*, 2008, **64**, 9230.

17 Y. Tao, Q. Wang, C. Yang, Q. Wang, Z. Zhang, T. Zou, J. Qin and D. Ma, *Angew. Chem., Int. Ed.*, 2008, **47**, 8104.

18 (*a*) Z. Zhang, Y. Zhang, D. Yao, H. Bi, I. Javed, Y. Fan, H. Zhang and Y. Wang, *Cryst. Growth Des.*, 2009, **9**, 5069; (*b*) Z. Zhang, R. M. Edkins, J. Nitsch, K. Fucke, A. Eichhorn, A. Steffen, Y. Wang and T. B. Marder, *Chem.–Eur. J.*, 2015, **21**, 177; (*c*) X. Wang, Q. Liu, H. Yan, Z. Liu, M. Yao, Q. Zhang, S. Gong and W. He, *Chem. Commun.*, 2015, **51**, 7497.

19 (*a*) Y. Tao, Q. Wang, Y. Shang, C. Yang, L. Ao, J. Qin, D. Ma and Z. Shuai, *Chem. Commun.*, 2009, 77; (*b*) Y. Tao, Q. Wang, L. Ao, C. Zhong, J. Qin, C. Yang and D. Ma, *J. Mater. Chem.*, 2010, **20**, 1759; (*c*) Y. Tao, Q. Wang, C. Yang, C. Zhong, J. Qin and D. Ma, *Adv. Funct. Mater.*, 2010, **20**, 2923.

20 V. Adamovich, J. Brooks, A. Tamayo, A. M. Alexander, P. I. Djurovich, B. W. D'Andrade, C. Adachi, S. R. Forrest and M. E. Thompson, *New J. Chem.*, 2002, **26**, 1171.

21 C. M. Cardona, W. Li, A. E. Kaifer, D. Stockdale and G. C. Bazan, *Adv. Mater.*, 2011, **23**, 2367.

22 (*a*) L. Deng, J. Li, G.-X. Wang and L.-Z. Wu, *J. Mater. Chem. C*, 2013, **1**, 8140; (*b*) X. Ouyang, D. Chen, S. Zeng, X. Zhang, S. Su and Z. Ge, *J. Mater. Chem.*, 2012, **22**, 23005; (*c*) Q. Li, L.-S. Cui, C. Zhong, Z.-Q. Jiang and L.-S. Liao, *Org. Lett.*, 2014, **16**, 1622.

23 (*a*) C.-J. Zheng, J. Ye, M.-F. Lo, M.-K. Fung, X.-M. Ou, X.-H. Zhang and C.-S. Lee, *Chem. Mater.*, 2012, **24**, 643; (*b*) W. Jiang, L. Duan, J. Qiao, G. Dong, L. Wang and Y. Qiu, *Org. Lett.*, 2011, **13**, 3146; (*c*) F.-M. Hsu, C.-H. Chien, Y.-J. Hsieh, C.-H. Wu, C.-F. Shu, S.-W. Liu and C.-T. Chen, *J. Mater. Chem.*, 2009, **19**, 8002; (*d*) S.-J. Su, E. Gonmori, H. Sasabe and J. Kido, *Adv. Mater.*, 2008, **20**, 4189.

24 J. P. Duan, P. P. Sun and C. H. Cheng, *Adv. Mater.*, 2003, **15**, 224.

25 B. C. Lin, C. P. Cheng, Z.-Q. You and C.-P. Hsu, *J. Am. Chem. Soc.*, 2005, **127**, 66.

26 X. Qiao, Y. Tao, Q. Wang, D. Ma, C. Yang, L. Wang, J. Qin and F. Wang, *J. Appl. Phys.*, 2010, **108**, 034508.

27 (*a*) C. Murawski, K. Leo and M. C. Gather, *Adv. Mater.*, 2013, **25**, 6801; (*b*) L. Zhu, Z. Wu, J. Chen and D. Ma, *J. Mater. Chem. C*, 2015, **3**, 3304.

28 (*a*) Y. Feng, P. Li, X. Zhuang, K. Ye, T. Peng, Y. Liu and Y. Wang, *Chem. Commun.*, 2015, **51**, 12544; (*b*) C.-H. Chen, L.-C. Hsu, P. Rajamalli, Y.-W. Chang, F.-I. Wu, C.-Y. Liao, M.-J. Chiu, P.-Y. Chou, M.-J. Huang, L.-K. Chu and C.-H. Cheng, *J. Mater. Chem. C*, 2014, **2**, 6183; (*c*) C.-H. Shih, P. Rajamalli, C.-A. Wu, M.-J. Chiu, L.-K. Chu and C.-H. Cheng, *J. Mater. Chem. C*, 2015, **3**, 1491.

29 T. Komino, H. Nomura, T. Koyanagi and C. Adachi, *Chem. Mater.*, 2013, **25**, 3038.

30 (*a*) *SHELXTL, version 5.1*, Siemens Industrial Automation, Inc., 1997; (*b*) G. M. Sheldrick, *SHELXS-97, Program for Crystal Structure Solution*, University of Göttingen, Göttingen, 1997.

31 E. Runge and E. K. U. Gross, *Phys. Rev. Lett.*, 1984, **52**, 997.

32 A. D. J. Becke, *Chem. Phys.*, 1993, **98**, 5648.

33 M. J. Frisch, G. W. Trucks, H. B. Schlegel, G. E. Scuseria, M. A. Robb, J. R. Cheeseman, J. A. Montgomery Jr, T. Vreven, K. N. Kudin, J. C. Burant, J. M. Millam, S. S. Iyengar, J. Tomasi, V. Barone, B. Mennucci, M. Cossi, G. Scalmani, N. Rega, G. A. Petersson, H. Nakatsuji, M. Hada, M. Ehara, K. Toyota, R. Fukuda, J. Hasegawa,

M. Ishida, T. Nakajima, Y. Honda, O. Kitao, H. Nakai, M. Klene, X. Li, J. E. Knox, H. P. Hratchian, J. B. Cross, C. Adamo, J. Jaramillo, R. Gomperts, R. E. Stratmann, O. Yazyev, A. J. Austin, R. Cammi, C. Pomelli, J. W. Ochterski, P. Y. Ayala, K. Morokuma, G. A. Voth, P. Salvador, J. J. Dannenberg, V. G. Zakrzewski, S. Dapprich, A. D. Daniels, M. C. Strain, O. Farkas, D. K. Malick, A. D. Rabuck, K. Raghavachari, J. B. Foresman, J. V. Ortiz, Q. Cui, A. G. Baboul, S. Clifford, J. Cioslowski, B. B. Stefanov, G. Liu, A. Liashenko, P. Piskorz, I. Komaromi, R. L. Martin, D. J. Fox, T. Keith, M. A. Al-Laham, C. Y. Peng, A. Nanayakkara, M. Challacombe, P. M. W. Gill, B. Johnson, W. Chen, M. W. Wong, C. Gonzalez and J. A. Pople, *Gaussian 03, Revision C.02*, Gaussian, Inc., Pittsburgh, PA, 2003.